EFFECT OF BAR TYPE ON THE PUNCHING SHEAR BEHAVIOUR OF GFRP-RC INTERIOR SLAB-COLUMN CONNECTIONS

Ahmed Gouda[1] and Ehab El-Salakawy[2]

[1] Ph.D. Student, Dept. of Civil Eng., University of Manitoba, Winnipeg, MB, Canada
[2] Professor and CRC, Dept. of Civil Eng., University of Manitoba, Winnipeg, MB, Canada

Abstract: This paper presents the results of an experimental program that was carried out to investigate the effect of bar type on the behaviour of interior slab-column connections. A total of three full-scale isolated Interior slab-column connections were constructed and tested to failure. One slab was reinforced with conventional steel bars, one with sand-coated GFRP bars and one with ribbed-deformed GFRP bars. The slabs were square with a side length of 2800 mm and a thickness of 200 mm. The central column had a 300-mm square section and extended above and below the slabs for a length of 1000 mm. The connections were subjected simultaneously to a vertical shear force and unbalanced moment, with a constant moment-to-shear ratio of 0.15 m. All test specimens failed due to punching shear of the central column through the slab. The test results showed that the slabs reinforced with sand-coated and ribbed-deformed GFRP bars had 25 and 33% lower capacity, respectively, compared to the steel reinforced one. In addition, the test results were compared to the shear provisions of the Canadian standard CSA/S806-12 and the American guideline ACI 440.1R-06 for the design of FRP-reinforced concrete structures.

1. Introduction

Flat plate structural system has many applications in the construction industry due to its numerous advantages, which include the simplified formwork, reduced storey heights and its ability to sustain heavy loads. Many of reinforced concrete (RC) parking garages in North America are constructed using flat plates supported directly on columns. These structures are subjected to severe environmental conditions, such as freeze-thaw cycles and de-icing salts, which may cause corrosion of steel and limit the life expectancy of the building. Using FRP bars as internal reinforcement in such structures would overcome the corrosion problem associated with the steel bars. On the other hand, the lack of sufficient experimental and analytical studies on the behaviour of flat slab system reinforced with FRP bars limits the knowledge and the full understanding of the behaviour of such slabs.

Punching shear failure in flat slab-column connections is a main concern for the designers, since it is sudden and brittle. This failure occurs due to the high transverse shear stresses caused by shear force and unbalanced moment transfer from the slab to the columns. This combination of shear and unbalanced moment is unavoidable at slab-column connections, due to unsymmetrical loading, unequal spans and effect of lateral loads, if any. Prevention of punching failure of slab-column connections depends on accurate calculations of shear stresses induced by shear forces and the unbalanced moments transferred to the columns. Also, the design and detailing of slab-column connections are critical to ensure the satisfactory performance of flat plat structures. The integrity of the whole structure is undermined if the joint where these members are connected fails.

Little research has been conducted on interior slab-column connections reinforced with FRP bars under concentric punching (Ospina et al. 2003; Hussein et al. 2004; Dulude et al. 2010 & 2013). The test variables in these researches were focusing on reinforcement ratio and column dimensions. It was mainly concluded that the punching failure will be affected by the bond characteristics and the elastic behaviour of the FRP reinforcement (Ospina et al. 2003). Hussein et al. 2004 reported that there was no apparent bond failure. Increasing the reinforcement ratio and perimeter-to-depth ratio decreased the deflections, reinforcement strains and increased the carrying load capacity (Dulude et al. 2013).

Also, Zaghloul (2002) tested six half-scale interior slab-column connections reinforced with CFRP grid under eccentric load. The test results revealed that increasing the column aspect ratio increased the carrying load capacity of the connection. However, none of these researches considered the effect of the unbalanced moment on the behaviour of full-scale slab-column connections reinforced with GFRP bars. The research program descried herein contributes to fulfilling this gap.

2. Experimental Program

2.1 Test Specimens

Three interior slab-column connections were constructed and tested to failure (SG, SR and SS). The main test variable was the type of reinforcing bars. An elastic analysis on a multi-story, multi-bay parking garage structure was performed to determine the dimensions of the specimens. The spacing between columns were taken equals to 6.5-m in both orthogonal directions. The typical specimen represented the zone of negative moment bounded by the lines of contra-flexure around an interior column. Each connection consisted of 2800 × 2800 × 200 mm slab with a 300-mm square column extended for 1000 mm above and below the slab. One slab (SG) was reinforced with sand-coated GFRP bars; one (SR) with ribbed-deformed GFRP bars and one (SS) with steel bars as control. No reinforcement was provided in the compression side of the slabs. All columns were reinforced with steel bars and stirrups to prevent premature failure. The dimensions and reinforcement details of a typical test specimen are shown in Figure 1.

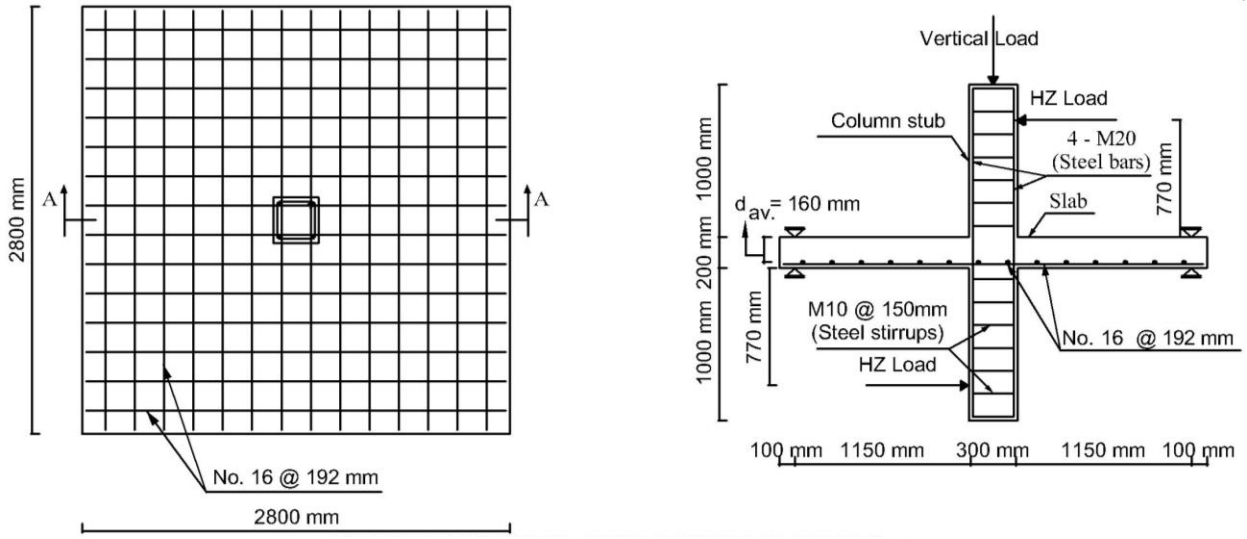

a) Typical reinforcement layout b) Section A-A

Figure 1 – Reinforcement configuration

2.2. Material properties

The connections were cast using normal weight, ready mixed concrete from a local supplier. The target compressive strength was 35 MPa, while, the actual compressive strength was determine on the day of testing for each connection by performing standard cylinder test (CSA/A23.2-14). In addition to regular G400 steel, two types of GFRP bars, sand-coated and ribbed-deformed, were used in this study. The properties of the used reinforcement are listed in Table 1.

Table 1 – Properties of reinforcing bars

Bar Type	Diameter (mm)	Area (mm2)	Tensile Modulus (GPa)	Ultimate Strength (MPa)	Ultimate Strain (%)
Sand-Coated GFRP	15.9	198	68.0	1398	2.05
Ribbed-Deformed GFRP	15.9	201	63.1	1122	1.78
Steel (G400)	15.9	200	200	f_y = 480*	ε_y = 0.24*

* Steel yield stress and strain, respectively.

2.3 Test setup

The test setup shown in Figure 2 was designed to test the specimens in upside down position with respect to the actual position of the real structure. The loads were applied axially and laterally to the tips of the column using a hydraulic actuator and two hydraulic jacks, respectively. The four edges of the slab were simply-supported on steel beams above and below the slab with all corners free to lift. The shearing force, *V*, (produced via the vertical actuator) and the unbalanced moment, *M*, (produced by the horizontal hydraulic jacks) were applied such that (*M*/*V*) = 0.15 m.

Figure 2 – Test Setup

2.4 Instrumentations

Deflections at several points along the two orthogonal slab centerlines were measured using 12 linear variable differential transducers (*LVDTs*). Also, electrical strain gauges were used to measure strains at 11 critical locations on the tension reinforcing mats in addition to two pi-gauges to measure the concrete strains.

3. Test results

3.1 Cracking and failure mode

The cracking load varied between 108 kN and 130 kN as shown in Table 2. The first crack in each slab was radial crack started from one of the corners of the column and extended to one of the edges of the slab. As the load increased, similar radial cracks propagated in the tension side of the slab with deferent inclination angles. The first tangential crack appeared around the column perimeter was approximately at 50% from the ultimate capacity of the connections. These cracking patterns are similar to the ones reported in the literature for the slabs reinforced with steel bars.

All connections failed in punching shear where the column with part of the slab penetrated through the slab thickness. The maximum concrete strain was less than 1000 micro-strains (Table 2) and no rupture happened in the reinforced bars, which confirm the shear failure. Figure 3 shows the cracks patterns of the tested slabs at failure.

Table 2 – Connections characteristics and results

Specimen	Concrete Compressive Strength, *fc'* (MPa)	First Crack Load (kN)	Maximum Deflection at Failure (mm)	Reinforcement Strain at Failure (με)	Max. Concrete Strain (με)	Post-Cracking Stiffness, K_P,(kN/mm)
SS	42	130	20.0	10369	-295	18.4
SG	42	116	28.4	8700	-515	6.7
SR	40	108	26.2	7111	-869	6.6

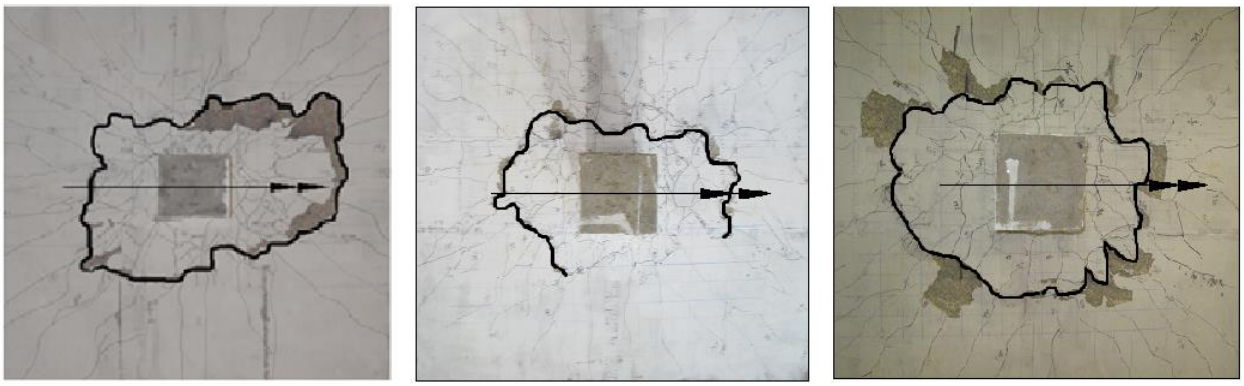

a) SG b) SR c) SS

Figure 3 – Crack patterns on the tension face of the slab at failure

3.2 Deflection

To consider the effect of the unbalanced moment, the service load was obtained from live load acting on half of the area (6.5 x 6.5 m) carried by the central column and dead load acting on the whole area (NBCC 2010). The obtained service load was 295 kN.

Figure 4 shows the maximum deflection in the slabs at 50 mm from the column face versus the vertical load. It can be seen from the figure that the load-deflection curve can be represented by two stages. The first stage represents the behaviour of the uncracked concrete while the second one depicts the stiffness of the cracked slabs. In the post cracking stage, the stiffness of the slabs was significantly different as it depends on the axial stiffness, $\rho_f E_f$, of the reinforcing bars. Therefore, the decrease in the stiffness was more pronounced in the GFRP-slabs, especially slab SR since it has the lowest modulus of elasticity among the three tested slabs.

The post-cracking stiffness, K_P, calculated as the slope of the load-deflection curve after cracking (listed in Table 2) for slab SS, was 174 and 178% higher than those of SG and SR, respectively. This resulted in a 203 and 243% increase in defection for slabs SG and SR compared to slab SS, respectively at the service load stage. These percentages decreased at failure to be 42 and 31%, respectively.

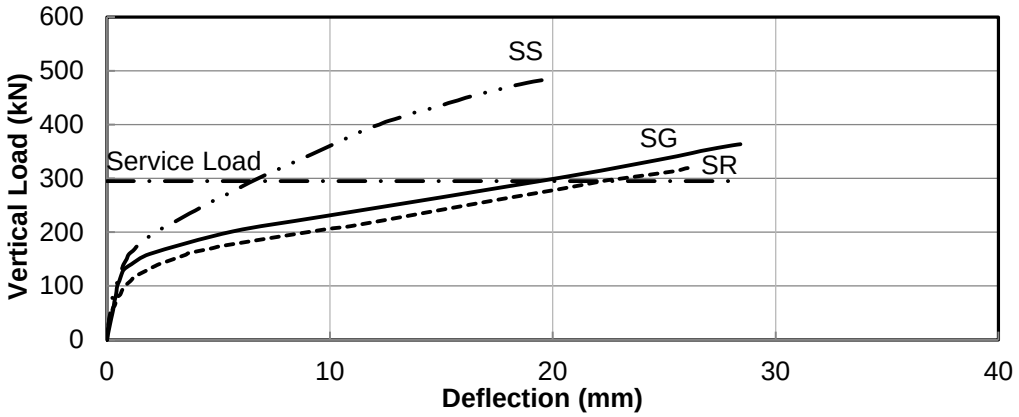

Figure 4 – Load-deflection relationship for test specimens

3.3 Strains

Figure 5 depicts the maximum strain in the reinforcing bars at the column face with the vertical load. In all slabs, the measured strain in the bars was insignificant up to the first crack. As the cracks extended in the slabs, the strain in the bars rapidly increased. The maximum reinforcement strain in slabs SG and SR was 8700 and 7111 με, respectively. This is approximately 42 and 43% of the ultimate strain of the sand-coated and ribbed-deformed GFRP bars, respectively.

Compared to the steel-RC slab, the slabs with GFRP bars exhibited higher strains at the same load level due to the low modulus of elasticity of the GFRP bars, which resulted in wider and deeper cracks. These wide cracks reduced the depth to neutral axis, which increased the strains in the GFRP bars. At service load level, the strains in slabs SG and SR were 384 and 327% higher than that of the steel-RC slab (SS), respectively. While at failure, these percentages were 16 and 31% less, respectively, due to the different capacity of the slabs and the yielding of the steel bars. The maximum measured strains in the bars are given in Table 2.

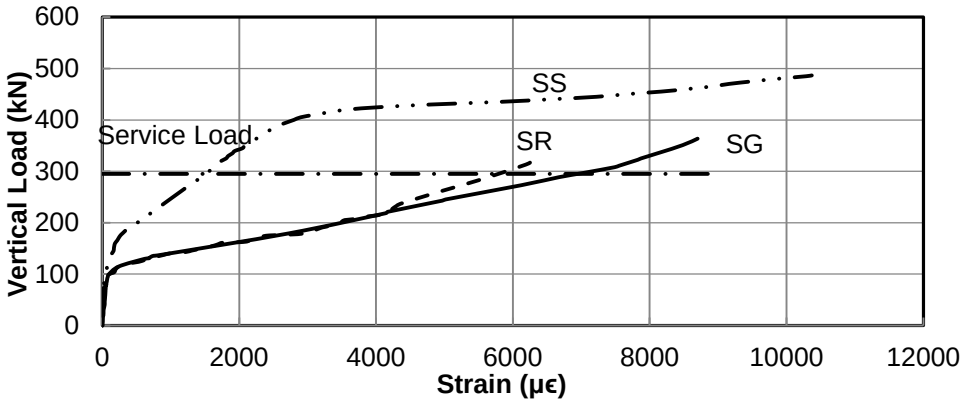

Figure 5 – Load-reinforcement strain relationship

3.4 Ultimate capacity

The failure loads for the slabs are listed in Table 3. To eliminate the effect of concrete compressive strength variations, the ultimate loads of slabs were multiplied by $\sqrt[3]{42/f_c'}$, The test results reveled that slabs SG and SR had 25 and 33% less capacity with reference to slab SS, respectively. This was mainly due to the higher elastic modulus of the steel bars with respect to the GFRP ones (Table 1). The low modulus of elasticity of the GFRP resulted in higher strain values in the bars, which caused wider and deeper cracks in the GFRP-slabs and reduced the shear capacity of those slabs (SG and SR) in terms of un-cracked concrete and aggregate interlock. Also, unlike steel bars, GFRP bars are uni-directional materials with low strength and stiffness in the transverse direction. This result in smaller dowel force and, consequently, less contribution shear resistance.

Table 3 - failure loads, punching shear stresses and Predicted loads

Specimen	Failure Loads, $V_{exp.}$ (kN)	$V_{exp.}\sqrt[3]{\frac{42\ (\mathrm{MPa})}{f_c'}}$ $V_{norm.}$ (kN)	Punching Shear Stresses (MPa)	CSA/S806-12 (2012) Predictions, (kN)		ACI 440.1R-06 (2006) Predictions, (kN)	
				$V_{CSA.}$	$V_{exp.}/V_{CSA.}$	$V_{ACI.}$	$V_{exp.}/V_{ACI.}$
SS	486	486	2.27	-	-	-	-
SG	363	363	1.70	316	1.15	172	2.11
SR	320	325	1.50	304	1.05	165	1.94
				Mean	1.10		2.02
				SD	0.05		0.08
				COV (%)	4.54		3.96

3.5 Code Comparison

The Canadian standard association published new code for FRP materials (CSA/S806-12); the code contains the following three equations to predict the punching load of the slabs. According to the code

provisions, the shear strength should be taken as the least value from the equations. In addition, the critical section should be taken at 0.5 *d* from the column faces, where *d* is the effective slab-depth.

$$v_c = 0.028\lambda\,\varphi_c\left(1+\frac{2}{\beta_c}\right)\left(E_f\rho_f f_c'\right)^{\frac{1}{3}} \quad \text{(MPa)} \quad [1]$$

$$v_c = 0.147\lambda\,\varphi_c\left(0.19+\alpha_s\frac{d}{b_o}\right)\left(E_f\rho_f f_c'\right)^{\frac{1}{3}} \quad \text{(MPa)} \quad [2]$$

$$v_c = 0.056\lambda\,\varphi_c\left(E_f\rho_f f_c'\right)^{\frac{1}{3}} \quad \text{(MPa)} \quad [3]$$

Where, v_c is the shear strength of concrete; λ is the concrete density factor; φ_c is the concrete resistance factor; β_c is the ratio of longer to shorter sides of the column; E_f is the elastic modulus for the FRP flexural reinforcement; ρ_f is the FRP flexural reinforcement ratio; f_c' is the concrete compressive strength (up to 60 MPa); $\alpha_s = 4$ for interior connections and b_o is the critical section perimeter.

Moreover, the American guideline for FRP materials (ACI 440.1R-06) gave only one equation to predict the ultimate capacity of the slabs.

$$V_c = \frac{4}{5}\sqrt{f_c'}\,b_o c \quad \text{(N)} \quad [4a]$$

$$\text{Where,} \quad c = kd \quad \text{(mm)} \quad [4b]$$

$$k = \sqrt{2\rho_f n_f + (\rho_f n_f)^2} - \rho_f n_f \quad [4c]$$

Where, V_c is the concrete nominal shear strength; f_c' is the concrete compressive strength; c is the depth of the neutral axis of the cracked transformed section; and n_f is the modular ratio.

Table 3 presents the predictions of the CSA/S806-12 standard (CSA 2012) and ACI 440.1R-06 (ACI 2006) guideline for the ultimate capacity of the GFRP-slabs. All the safety factors in the equations were set equal to unity. CSA/S806-12 code gave close prediction to the failure load with an average of $V_{exp.}/V_{CSA.} = 1.10 \pm 0.05$ (COV = 4.54%). On contrast, ACI 440.1R-06 guideline underestimated the capacity with an average of $V_{exp.}/V_{ACI.} = 2.02 \pm 0.08$ (COV = 3.96%).

The ACI guideline included the effect of the reinforcement ratio and the elastic modulus of the FRP bars in calculating the depth to neutral axis, *c*, while the direct implementation of the axial stiffness, $\rho_f E_f$, of the reinforcing bars in the prediction equations yielded better results as seen in the Canadian code predictions.

4. Conclusion

The behaviour of three full-scale interior slab-column connections, tested under eccentric load with 0.15-m moment-to-shear ratio, was evaluated. Based on the test results discussed herein, the following could be concluded.

1- All test slabs failed in punching shear, where the column with part of the slab penetrated through the slab-thickness.
2- Slabs reinforced with GFRP bars had higher deflections and reinforcement strains with reference to the steel-RC slab. At service load level, slabs SG and SR exhibited 203 and 243% higher deflections than that of the reference slab SS, respectively.

3- The axial stiffness of the reinforcing bars significantly affects the behaviour of the slabs. The slabs reinforced with sand-coated (SG) and ribbed-deformed (SR) GFRP bars had 25 and 33% less punching load with respect to the steel-RC slab (SS), respectively, due to the lower elastic modulus of the GFRP bars.
4- The Canadian standard CSA/S806-12 (CSA 2012) gave reasonable, yet conservative, predictions to the experimental failure loads of the slabs with an average of $V_{exp.}/V_{CSA.} = 1.10 \pm 0.05$ (COV = 4.54%). However, the American design guideline ACI 440.1R-06 (ACI 2006) highly underestimated the failure loads of the slabs with an average of $V_{exp.}/V_{ACI.} = 2.02 \pm 0.08$ (COV = 3.96%).

5. Acknowledgements

The authors wish to express their sincere gratitude to the Natural Sciences and Engineering Council of Canada (NSERC) through Discovery and Canada Research Chairs Programs. The assistance received from the technical staff of the McQuade Structures Laboratory is acknowledged. Also, the ribbed-deformed GFRP reinforcement generously provided by Schoeck Canada Inc. is greatly appreciated.

6. References

ACI Committee 440. 2006. Guide for the Design and Construction of Concrete Reinforced with FRP Bars (ACI 440.1R-06). *American Concrete Institute*, USA, 44 p.

CAN/CSA A23.2-14. 2014. Method of Test for Concrete. *Canadian Standards Association*, Rexdale, Ontario, Canada, 203 p.

CAN/CSA S806-12. 2012. Design and Construction of Building Components with Fibre-Reinforced Polymers. *Canadian Standards Association*, Rexdale, Ontario, Canada, 187 p.

Canadian Commission on Building and Fire Codes. 2010. National Building Code of Canada*. National Research Council of Canada, (NRCC), Ottawa,* Ontario, Vol. 2.

DULUDE, C. AHMED, E. and BENMOKRANE, B. 2010. Punching Shear Strength of Concrete Flat Slabs Reinforced with GFRP Bars. *2nd International Structures Specialty Conference*, (CSCE), Winnipeg, Manitoba, Canada, 9 p.

DULUDE, C. HASSAN, M. AHMED, E. and BENMOKRANE, B. 2013. Punching Shear Behavior of Flat Slabs Reinforced with Glass Fiber-Reinforced Polymer Bars. *ACI Structural Journal*, 10: 723-734.

HUSSEIN, A. RASHID, M. and BENMOKRANE, B. 2004. Two–Way Concrete Slabs Reinforced with GFRP Bars. *Advanced Composite Materials in Bridges and Structures,* (ACMBS), Calgary, Alberta, Canada, 8 p.

OSPINA, C. ALEXANDER, S. and CHENG, J. 2003. Punching of Two-Way Concrete Slabs with Fiber-Reinforced Polymer Reinforcing Bars or Grids. *ACI Structural Journal*, 100: 589-598.

ZAGHLOUL, A. 2002. Behaviour and strength of CFRP-reinforced flat plate interior column connections subjected to shear and unbalanced moments. *Master's thesis*, Carleton University.